

Joint Prefiltering and MLSE Equalization of Space-Time-Coded Transmissions over Frequency-Selective Channels

Waleed Younis ^{*}and Naofal Al-Dhahir [†]

Abstract

The problem of designing a front-end prefilter to improve the performance and/or reduce the complexity of MLSE equalization of space-time-coded signals is addressed in this paper. The front-end prefilter performs channel shortening without excessive noise enhancement and is constrained to be an FIR filter for practical implementation. Transmission scenarios emphasized assume 2 transmit antennas (with delay diversity or space-time trellis coding) and either 1 or 2 receive antennas. Extensions to more antennas are straightforward. Various design parameters (such as number of prefilter taps, number of equalizer states, and decision delay) are optimized using Monte Carlo simulations in a Typical Urban EDGE environment.

1 Introduction

Transmitter diversity has been proposed for third generation cellular standards such as CDMA-2000 [1] and W-CDMA [2] due to its effectiveness against multipath fading by employing multiple transmit antennas at the base station rather than at the mobile terminal which is desired to have low complexity. The successful application of transmitter diversity to the proposed third generation TDMA standard known as EDGE requires the development of effective and practical equalization schemes to combat the severe intersymbol interference (ISI) effects due to frequency selectivity of the wideband 200 kHz multiple transmission channels and the Gaussian transmit filter.

Although maximum likelihood sequence estimation (MLSE) [3] is a well-established effective equalization scheme for ISI channels, its complexity (as measured by the number of trellis states) is too high for practical implementation in EDGE, especially with multiple transmit antennas and large signal constellations (to achieve higher spectral efficiencies). More specifically, the number of MLSE states

^{*}W. Younis is with the EE Dept., University of California, Los Angeles, CA 90095. This work was performed while Waleed was at AT&T Shannon Laboratory during Summer 2000

[†]Naofal Al-Dhahir is with AT&T Shannon Laboratory, 180 Florham Park, NJ 07932, Email: naofal@research.att.com

required in general is $M^{n_i \nu}$ where M is the signal constellation size, n_i is the number of transmit antennas, and ν is the memory of the overall channel impulse response (CIR)¹. For the EDGE Typical Urban (TU) channel, $\nu \approx 3$. Using the 8-PSK modulation scheme adopted for EDGE with 2 transmit antennas results in $8^6 = 262144$ equalizer states; which is clearly of prohibitive complexity. Suboptimum equalization techniques such as linear and decision feedback equalization (DFE) can be used to reduce the implementation complexity but at the expense of performance degradation due to noise enhancement and error propagation, respectively. An attractive equalization scheme that represents a tradeoff between DFE and MLSE is delayed decision feedback sequence estimation (DDFSE) introduced in [4]. In DDFSE, the memory of the channel is divided into two parts; the first part is used to construct a trellis based on which an MLSE equalizer is constructed and the second part of the channel memory is cancelled by hard decision feedback. Hence, DDFSE is a hybrid of DFE and MLSE. The optimum front-end prefilter (FEP) for DDFSE in the single-transmit single-receive scenario is the whitened matched filter (WMF) [3, 4] which converts the original overall CIR to a *minimum-phase* impulse response whose energy is concentrated in its leading samples; thus minimizing error propagation effects in DDFSE. However, the WMF is of infinite length in general. An FIR implementation is required in practice, which makes the assumption of a minimum-phase response at the WMF output not true in general, causing degradation in DDFSE performance. In addition, the use of multiple transmit antennas results in multiple transmission channels that need to be *simultaneously* converted to minimum phase making the FEP design even more challenging. The FEP design problem with transmit diversity and (optional) receive diversity is studied in this paper. Previous work on DDFSE equalization for transmit diversity signaling has been reported in [5] where a 64-state DDFSE is used with no FEP. The organization of this paper is as follows. In Section 2, we describe the two transmit diversity schemes and the DDFSE equalization scheme considered in this paper. The FEP design problem is formulated and solved in Section 3 for single/multiple transmit/receive antennas. Extensive simulation results are presented in Section 4 and the paper is concluded in Section 5.

2 Equalization & Transmit Diversity for EDGE

In this section, we describe the two transmit diversity schemes and the equalization algorithms studied in this paper.

¹By overall CIR, we mean the convolution of the transmit pulse shape and the physical multipath channel.

2.1 Transmit Diversity

Spatial transmit diversity, and in particular space–time coding, has received considerable attention recently from researchers due to its many advantages. First, it improves the downlink performance (which is the bottleneck in asymmetric data services such as internet access) without the need for multiple receive antennas at the terminals (which are required to have low cost and a small form factor). Second, it can be elegantly combined with channel coding, as shown in [6], realizing a coding gain in addition to the diversity gain. Third, they do not require channel state information (CSI) at the transmitter, i.e. operate in open–loop mode, thus eliminating the need for an expensive, and unreliable in case of rapid channel fading, reverse link. Finally, they have been shown to be robust against non–ideal operating conditions such as antenna correlation, channel estimation errors, and Doppler effects [7, 8].

The scenario of transmit diversity over a frequency–selective Rayleigh fading channel with n_i transmit antennas and n_o receive antennas is depicted in Figure 1. The m^{th} impulse response coefficient of the overall channel from transmit antenna i to receive antenna j is denoted by $h_{ij}(m)$. The channel memory, denoted by ν , is assumed the same for all channels. The received signal at time k at the j^{th} receive antenna, denoted by $r_j(k)$, is given by

$$r_j(k) = \sum_{i=1}^{n_i} \sum_{m=0}^{\nu} h_{ij}(m) x_i(k-m) + n_j(k) , \quad (1)$$

where $x_i(k)$ is the signal transmitted from the i^{th} antenna at time k , and $n_j(k)$ is the noise at the j^{th} receive antenna. The samples from all n_o receive antennas can be grouped into an $n_o \times 1$ column vector $\mathbf{r}(k)$ as follows

$$\mathbf{r}(k) = \sum_{m=0}^{\nu} \mathbf{h}(m) \mathbf{x}(k-m) + \mathbf{n}(k) , \quad (2)$$

where $\mathbf{h}(m)$ is the multiple–input multiple–output (MIMO) channel matrix coefficient at time m of size $n_o \times n_i$, $\mathbf{x}(k-m)$ is the input vector at time $k-m$ of size $n_i \times 1$, and $\mathbf{n}(k)$ is the noise vector of size $n_o \times 1$ at time k . The noise is assumed independent of the input, Gaussian distributed, and has a positive–definite auto–correlation matrix \mathbf{R}_{nn} .

In this paper, we focus on transmit diversity with two transmit antennas using delay diversity or the 8–state 8–PSK space–time trellis code (STTC) and one or two receive antennas. It has been shown in [5] that the special structure of these codes can be exploited to reduce the complexity of the equalizer.

2.1.1 Delay Diversity

In delay diversity transmission with 2 antennas, the signal transmitted from the second antenna is a delayed version of the signal transmitted from the first antenna. To reduce receiver complexity, we limit ourselves in this paper to a delay of one symbol period. The received signal with n_o receive antennas is given by

$$\mathbf{r}(k) = \sum_{m=0}^{\nu+1} \mathbf{h}_{eqv}^{DD}(m) x_1(k-m) + \mathbf{n}(k) , \quad (3)$$

where $\mathbf{h}_{eqv}^{DD}(m)$ is the m^{th} vector coefficient (of size $n_o \times 1$) of the equivalent single-input single-output (SISO) CIR for delay diversity transmission whose D-transform is given by

$$\mathbf{h}_{eqv}^{DD}(D) = \mathbf{h}_1(D) + D\mathbf{h}_2(D) . \quad (4)$$

In the above equation, $\mathbf{h}_l(D) = [h_{l1}(D) \ \cdots \ h_{ln_o}(D)]^t$ for $l = 1, 2$ and $(.)^t$ is the transpose operator. Therefore, a 2-transmit 1-receive delay diversity transmission over 2 dispersive channels each of memory ν is equivalent to a 1-transmit 1-receive transmission over an equivalent SISO dispersive channel of memory $(\nu + 1)$. In other words, spatial diversity is transformed to temporal (multipath) diversity whose gain is realized at the receiver by effective equalization of the equivalent SISO channel. The price paid is an increase, by a factor of M , in the number of equalizer states required ² *when full-complexity MLSE equalization is used*. Reduced-complexity equalization schemes for delay diversity are studied in Section 3.1.

2.1.2 8-State 8-PSK Space-Time Trellis Code

The trellis description of the 8-state 8-PSK STTC for 2 transmit antennas is given in Figure 7 of [6]. It can be readily verified that this transmission scheme is identical to delay diversity *except* that the delayed symbol from the second antenna is multiplied by -1 if it is an odd symbol, i.e. $\in \{1, 3, 5, 7\}$. This slight modification results in an additional coding gain of 2.5 dB over a Rayleigh flat-fading channel [6].

The received signal for the 8-state 8-PSK STTC case with n_o receive antennas is given by

$$\mathbf{r}(k) = \sum_{m=0}^{\nu+1} \mathbf{h}_{eqv}^{STTC}(m) x_1(k-m) + \mathbf{n}(k) , \quad (5)$$

where \mathbf{h}_{eqv}^{STTC} is the equivalent time-varying SISO CIR vector for the STTC case whose D-transform

²Compared to the scenario of SISO transmission over $h_1(D)$ only.

is given by

$$\mathbf{h}_{eqv}^{STTC}(k, D) = \mathbf{h}_1(0) + \sum_{m=1}^{\nu} (\mathbf{h}_1(m) + s_k \mathbf{h}_2(m-1)) D^m + \mathbf{h}_2(\nu) D^{\nu+1}, \quad (6)$$

where $s_k = \pm 1$ is data-dependent. The main attractive feature of the equivalent channel representation in (6) is that the encoder structure is embedded in the CIR. Hence, joint space-time equalization and decoding can be performed using a single trellis based on this equivalent channel as opposed to two separate trellises for equalization and decoding. Exploiting the structure of the space-time code in this manner translates into significant savings in implementation complexity.

2.2 Delayed Decision Feedback Sequence Estimation

The branch metric of the received signal at time k of the MLSE equalizer for STTC is given by

$$\xi(k) = \left\| \mathbf{r}(k) - \sum_{i=0}^{\nu+1} \mathbf{h}_{eqv}^{STTC}(i) \tilde{s}(k-i) \right\|^2, \quad (7)$$

where \mathbf{h}_{eqv}^{STTC} is the equivalent channel given by (6) and $\tilde{s}(k)$ are all possible symbols according to different transitions along the path history. MLSE complexity increases exponentially with the channel memory. A tradeoff between complexity and performance can be achieved by using DDFSE to reduce the number of MLSE states. In this case, the branch metric is given by

$$\xi(k) = \left\| \mathbf{r}(k) - \sum_{i=0}^n \mathbf{h}_{eqv}^{STTC}(i) \tilde{s}(k-i) - \sum_{i=n+1}^{\nu+1} \mathbf{h}_{eqv}^{STTC}(i) \hat{s}(k-i) \right\|^2, \quad (8)$$

where n is a design parameter ($0 \leq n \leq \nu$) that determines the number of DDFSE trellis states and $\hat{s}(k)$ are the previous hard symbol decisions along the path history. DDFSE assumes that these symbols are decoded correctly and uses them to equalize the effect of the discarded trellis states. From (8), we can see that DDFSE can be considered as a combination of MLSE and DFE that uses a state description of the channel to recursively estimate the best path in the trellis while storing only one path for each state as in MLSE. However, in the DDFSE case, each state (which corresponds to n symbols of channel memory) provides only partial information about the full state of the channel. In order to cancel the interference from the past symbols occurring earlier than n symbols in the past, hard feedback information is extracted from the best path.

3 Front-End Prefilter Design

In general, the role of the FEP is to reshape the effective CIR seen by the DDFSE to improve its BER or reduce its complexity or both. In this paper, the FEP is designed to be an FIR filter that shortens the effective CIR under the following additional requirements :

1. The signal energy over a desired time window at the output of the FEP is maximized to achieve good signal distance properties.
2. The signal energy outside the desired time window at the output of the FEP is minimized to reduce error propagation effects in DDFSE and signal energy loss.
3. Any noise energy enhancement by FEP is minimized. However, the noise samples at the FEP output will be correlated. We chose not to include this noise correlation in the DDFSE metric calculations (c.f. Equation (8)) to reduce receiver complexity at the expense of some performance loss.

An algorithm that achieves the first and second requirements above was first reported in [9] and refined in [10]. We selected the algorithm in [10] for FEP design and extended it in the following 3 ways :

1. Included noise level in FEP design to meet Requirement (3) above and to improve the numerical behavior of the algorithm as it will be illustrated in Section 4.
2. Extended it to the multi-channel case which is needed for the 8-State 8-PSK STTC transmission scenario.
3. Extended it to the multiple-receive-antenna case (see Section 3.3).

3.1 Delay Diversity Case

We showed in Subsection 2.1.1 that, as far as the receiver is concerned, transmit delay diversity is equivalent to SISO transmission over a modified CIR with longer memory. Therefore, the SISO channel-shortening algorithm in [9, 10] can be applied to delay diversity systems. In this subsection, we briefly review this algorithm, modify it to include noise effects, and apply it to transmit delay diversity. Denote the convolution of the original length- $(\nu + 1)$ CIR \mathbf{h} and the length- N_f FEP \mathbf{w} by the length- $(N_f + \nu)$ effective CIR \mathbf{h}_{eff} . Then, it can be readily checked that

$$\mathbf{h}_{eff} = \mathbf{H}\mathbf{w} , \tag{9}$$

where the $(N_f + \nu) \times N_f$ Toeplitz convolution matrix \mathbf{H} is given by

$$\mathbf{H} = \begin{bmatrix} h(0) & 0 & \cdots & 0 \\ h(1) & h(0) & \ddots & \vdots \\ \vdots & h(1) & \ddots & 0 \\ h(\nu) & \vdots & \ddots & h(0) \\ 0 & h(\nu) & \ddots & h_1 \\ \vdots & 0 & \ddots & \vdots \\ 0 & 0 & \cdots & h(\nu) \end{bmatrix}.$$

Let \mathbf{h}_{win} denote a window of $(N_b + 1)$ consecutive samples of \mathbf{h}_{eff} , assuming a delay of Δ samples (where $0 \leq \Delta \leq N_f + \nu - N_b - 1$), and let \mathbf{h}_{wall} denote the remaining samples of \mathbf{h}_{eff} . Using compact matrix notation, we can express \mathbf{h}_{win} and \mathbf{h}_{wall} as follows

$$\mathbf{h}_{win} = \left[\mathbf{e}_{\Delta+1} \cdots \mathbf{e}_{\Delta+N_b+1} \right]^t \mathbf{h}_{eff} \quad (10)$$

$$\mathbf{h}_{wall} = \left[\mathbf{e}_1 \cdots \mathbf{e}_{\Delta} \mathbf{e}_{\Delta+N_b+2} \cdots \mathbf{e}_{N_f+\nu} \right]^t \mathbf{h}_{eff}, \quad (11)$$

where \mathbf{e}_i is the i^{th} unit column vector of size $(N_f + \nu)$. The FEP coefficients are computed by *maximizing* the ratio of the channel energy in \mathbf{h}_{win} to the sum of the channel energy in \mathbf{h}_{wall} *plus* the noise energy at the FEP output. Mathematically, we solve the following optimization problem [9, 10]

$$\begin{aligned} \max_{\mathbf{w}} \mathbf{h}_{win}^* \mathbf{h}_{win} &\equiv \max_{\mathbf{w}} \mathbf{w}^* \mathbf{H}^* \text{diag}(\mathbf{0}_{\Delta}, \mathbf{1}_{(N_b+1)}, \mathbf{0}_{(N_f+\nu-N_b-\Delta-1)}) \mathbf{H} \mathbf{w} \\ &\stackrel{def}{\equiv} \max_{\mathbf{w}} \mathbf{w}^* \mathbf{H}_{win}^* \mathbf{H}_{win} \mathbf{w} \stackrel{def}{\equiv} \max_{\mathbf{w}} \mathbf{w}^* \mathbf{B} \mathbf{w}, \end{aligned} \quad (12)$$

subject to the condition

$$\mathbf{h}_{wall}^* \mathbf{h}_{wall} + \mathbf{w}^* \mathbf{R}_{nn} \mathbf{w} = 1$$

which can be expressed as follows

$$\begin{aligned} \mathbf{h}_{wall}^* \mathbf{h}_{wall} + \mathbf{w}^* \mathbf{R}_{nn} \mathbf{w} &= 1 \\ \mathbf{w}^* \mathbf{H}^* \text{diag}(\mathbf{1}_{\Delta}, \mathbf{0}_{(N_b+1)}, \mathbf{1}_{(N_f+\nu-N_b-\Delta-1)}) \mathbf{H} \mathbf{w} + \mathbf{w}^* \mathbf{R}_{nn} \mathbf{w} &= 1 \\ \Leftrightarrow \mathbf{w}^* \mathbf{H}_{wall}^* \mathbf{H}_{wall} \mathbf{w} &= 1 \\ \Leftrightarrow \mathbf{w}^* \mathbf{A} \mathbf{w} &= 1, \end{aligned} \quad (13)$$

where $\text{diag}(\cdot)$ denotes a diagonal matrix, $\mathbf{1}_l$ is the all-ones vector of size l , $\mathbf{0}_n$ is the all-zeros vector of size n , $\mathbf{B} \stackrel{def}{=} \mathbf{H}^* \text{diag}(\mathbf{0}_{\Delta}, \mathbf{1}_{(N_b+1)}, \mathbf{0}_{(N_f+\nu-N_b-\Delta-1)}) \mathbf{H} \stackrel{def}{=} \mathbf{H}_{win}^* \mathbf{H}_{win}$, and $\mathbf{A} \stackrel{def}{=} \mathbf{H}^* \text{diag}(\mathbf{1}_{\Delta}, \mathbf{0}_{(N_b+1)}, \mathbf{1}_{(N_f+\nu-N_b-\Delta-1)}) \mathbf{H} + \mathbf{R}_{nn} = \mathbf{H}_{wall}^* \mathbf{H}_{wall} + \mathbf{R}_{nn}$ is a Hermitian positive-definite matrix (hence invertible).

Define the Cholesky factorization [11] $\mathbf{A} = \mathbf{L}_A \mathbf{L}_A^*$, where \mathbf{L}_A is a lower-triangular matrix. Then, it can be shown [9, 10] that the optimum FEP coefficients are given by

$$\mathbf{w}_{opt} = (\mathbf{L}_A^*)^{-1} \mathbf{u}_{max} , \quad (14)$$

where \mathbf{u}_{max} is the orthonormal eigenvector of the matrix $(\mathbf{L}_A)^{-1} \mathbf{B} (\mathbf{L}_A^*)^{-1}$ corresponding to its largest eigenvalue λ_{max} . The Shortening Signal to Noise ratio (SSNR) is defined as follows [9, 10]

$$SSNR_{opt} \stackrel{def}{=} 10 \log \left(\frac{\mathbf{w}_{opt}^* \mathbf{B} \mathbf{w}_{opt}}{\mathbf{w}_{opt}^* \mathbf{A} \mathbf{w}_{opt}} \right) = 10 \log (\lambda_{max}) . \quad (15)$$

This FEP design algorithm can be readily applied to transmit delay diversity by setting $\mathbf{h} = \mathbf{h}_{equiv}^{DD}$ (c.f. Equation (4)).

Two remarks on the computational complexity of (14) are now in order. First, since the matrices \mathbf{A} and \mathbf{B} depend on Δ , it seems that an exhaustive search for the optimum Δ (that minimizes BER) is needed. We show by simulations in Section 4, that for the EDGE TU channel, such a search is not needed. Second, computationally-efficient algorithms for Cholesky factorization that utilize the structure of \mathbf{A} can be developed using the theory in [12]. Furthermore, \mathbf{u}_{max} can be computed iteratively using one of several numerical methods such as the *power method* [11]. We conclude this subsection by noting that the algorithms in [9, 10] do not include the noise term $\mathbf{w}^* \mathbf{R}_{nn} \mathbf{w}$ in the FEP design. This could result in numerical precision problems when computing $(\mathbf{L}_A^*)^{-1}$ in (14) as it will be illustrated in Section 4.

3.2 8-State 8-PSK STTC Case

We showed in Section 2 that the equivalent CIR for the delay diversity case with 2 transmit antennas and 1 receive antenna is a SISO channel that is 1 tap longer. However, for STTC, the equivalent SISO channel is data-dependent and hence time-varying (c.f. Equation (6)). Consequently, the FEP for the equivalent CIR has to be an adaptive filter that tracks the data-dependent channel time variations, which is very difficult to achieve in practice. In this section, we provide an alternative approach for prefiltering in the STTC case, without using a time-varying FEP, based on an extension of the technique described in Section 3.1. The block diagram of the proposed system is shown in Figure 2. A single FEP is designed to shorten both channels simultaneously based on a (modified) SSNR maximization criterion. The convolution of the 2 original CIRs and the single FEP results in the 2 effective channels $\mathbf{h}_{i_{eff}}$ (for $i = 1, 2$) each of length $(N_f + \nu)$. In matrix notation

$$\mathbf{h}_{i_{eff}} = \mathbf{H}_i \mathbf{w} , \quad (16)$$

where \mathbf{H}_i is given by

$$\mathbf{H}_i = \begin{bmatrix} h_i(0) & 0 & \cdots & 0 \\ h_i(1) & h_i(0) & 0 & \vdots \\ \vdots & h_i(1) & \ddots & 0 \\ h_i(\nu) & \vdots & \ddots & h_i(0) \\ 0 & h_i(\nu) & \ddots & h_i(1) \\ \vdots & 0 & \ddots & \vdots \\ 0 & 0 & \cdots & h_i(\nu) \end{bmatrix}. \quad (17)$$

Let $\mathbf{h}_{i_{win}}$ denote a time window of length N_{b_i} with a delay of Δ_i samples and $\mathbf{h}_{i_{wall}}$ denote the remaining samples of $\mathbf{h}_{i_{eff}}$. In matrix notation, $\mathbf{h}_{i_{win}}$ and $\mathbf{h}_{i_{wall}}$ can be expressed as follows

$$\begin{aligned} \mathbf{h}_{i_{win}} &= \begin{bmatrix} \mathbf{e}_{\Delta_i+1} & \cdots & \mathbf{e}_{\Delta_i+N_{b_i}+1} \end{bmatrix}^t \mathbf{h}_{i_{eff}} \\ &= \begin{bmatrix} \mathbf{e}_{\Delta_i+1} & \cdots & \mathbf{e}_{\Delta_i+N_{b_i}+1} \end{bmatrix}^t \mathbf{H}_i \mathbf{w} \\ &\stackrel{def}{=} \mathbf{H}_{i_{win}} \mathbf{w} \end{aligned} \quad (18)$$

$$\begin{aligned} \mathbf{h}_{i_{wall}} &= \begin{bmatrix} \mathbf{e}_1 & \cdots & \mathbf{e}_{\Delta_i} & \mathbf{e}_{\Delta_i+N_{b_i}+2} & \cdots & \mathbf{e}_{N_f+\nu-1} \end{bmatrix}^t \mathbf{h}_{i_{eff}} \\ &= \begin{bmatrix} \mathbf{e}_1 & \cdots & \mathbf{e}_{\Delta_i} & \mathbf{e}_{\Delta_i+N_{b_i}+2} & \cdots & \mathbf{e}_{N_f+\nu-1} \end{bmatrix}^t \mathbf{H}_i \mathbf{w} \end{aligned} \quad (19)$$

$$\stackrel{def}{=} \mathbf{H}_{i_{wall}} \mathbf{w}. \quad (20)$$

The FEP coefficients are optimized such that the sum of the total channel energy in $\mathbf{h}_{i_{win}}$ to the sum of the total channel energy in $\mathbf{h}_{i_{wall}}$ plus the noise energy at the FEP output is maximized. The mathematical formulation of this optimization problem is the same as in Section 3.1 with \mathbf{A} and \mathbf{B} now defined as follows

$$\mathbf{A} \stackrel{def}{=} \sum_{i=1}^2 \mathbf{H}_{i_{wall}}^* \mathbf{H}_{i_{wall}} + \mathbf{R}_{nn} \quad (21)$$

$$\mathbf{B} \stackrel{def}{=} \sum_{i=1}^2 \mathbf{H}_{i_{win}}^* \mathbf{H}_{i_{win}}. \quad (22)$$

The coefficients of the optimum FEP are again given by (14). It is important to note that the matrices \mathbf{A} and \mathbf{B} used in the FEP design are *not* data dependent. Hence, our design avoids the need for an adaptive FEP to shorten the equivalent time-varying channel $\mathbf{h}_{equiv}^{STTC}$ by instead prefiltering both channels simultaneously with a single FEP. This approach can also control the length of each shortened channel independently. The benefit of shortening the two channels to different lengths will become clear in Section 4. We conclude this subsection by mentioning that after prefiltering, the equivalent channel presented to DDFSE will have the SISO data-dependent form given in (6) *except* that \mathbf{h}_1

and \mathbf{h}_2 are replaced by their shortened counterparts $\mathbf{h}_{1_{eff}}$ and $\mathbf{h}_{2_{eff}}$, respectively. We emphasize that for the STTC case, the data-dependent channel model is used for equalizer design only while the 2-transmit 1-receive time-invariant channel model is used for FEP design.

3.3 Multiple Receive Antennas

Increasing the number of receiver antennas for transmit diversity systems improves the performance of the overall system due to the increased diversity order. In this section, we extend our FEP design to accommodate multiple-receiver-antenna systems. The system diagram for two-transmit two-receive system is shown in Figure 3. The problem in this case can be formulated mathematically as follows

$$\max_{\mathbf{w}_j} \mathbf{w}_j^* \mathbf{B}_j \mathbf{w}_j \quad \text{subject to the condition} \quad \mathbf{w}_j^* \mathbf{A}_j \mathbf{w}_j = 1 \quad \text{for } j = 1, 2, \dots, n_o \quad (23)$$

where \mathbf{w}_j is the impulse response of the FEP at the j^{th} receive antenna and \mathbf{B}_j and \mathbf{A}_j are defined as

$$\mathbf{B}_j \stackrel{def}{=} \sum_{i=1}^2 \mathbf{H}_{ij_{win}}^* \mathbf{H}_{ij_{win}} \quad (24)$$

$$\mathbf{A}_j \stackrel{def}{=} \sum_{i=1}^2 \mathbf{H}_{ij_{wall}}^* \mathbf{H}_{ij_{wall}} + \mathbf{R}_{nn}, \quad (25)$$

where \mathbf{H}_{ij} is the Toeplitz convolution matrix (has similar form to (17)) whose first column is $\left[h_{ij}(0) \ h_{ij}(1) \ \dots \ h_{ij}(\nu) \ \mathbf{0}_{1 \times (N_f - 1)} \right]^t$ and its two submatrices $\mathbf{H}_{ij_{win}}$ and $\mathbf{H}_{ij_{wall}}$ are defined as

$$\begin{aligned} \mathbf{H}_{ij_{win}} &= \left[\mathbf{e}_{\Delta_i+1} \ \dots \ \mathbf{e}_{\Delta_i+N_{b_i}+1} \right]^t \mathbf{H}_{ij} \\ \mathbf{H}_{ij_{wall}} &= \left[\mathbf{e}_1 \ \dots \ \mathbf{e}_{\Delta_i} \ \mathbf{e}_{\Delta_i+N_{b_i}+2} \ \dots \ \mathbf{e}_{N_f+\nu-1} \right]^t \mathbf{H}_{ij} \end{aligned}$$

Finally, the optimum FEP coefficients are obtained from the solution of (23) and are given by

$$\mathbf{w}_{j_{opt}} = \left(\mathbf{L}_{\mathbf{A}_j} \right)^{-1} \mathbf{u}_{j_{max}} \quad : \quad \text{for } j = 1, 2, \dots, n_o, \quad (26)$$

where $\mathbf{u}_{j_{max}}$ is the orthonormal eigenvector that corresponds to the maximum eigenvalue of the matrix $\left(\mathbf{L}_{\mathbf{A}_j} \right)^{-1} \mathbf{B}_j \left(\mathbf{L}_{\mathbf{A}_j}^* \right)^{-1}$ and we have defined the Cholesky factorization $\mathbf{A}_j \stackrel{def}{=} \mathbf{L}_{\mathbf{A}_j} \mathbf{L}_{\mathbf{A}_j}^*$.

4 Simulation Results

For our computer simulation, we consider the Typical Urban (TU) EDGE channel (whose power delay profile is given in Table 1). The overall CIR length is effectively 4 symbol periods; i.e., $\nu = 3$. In EDGE, fading can be safely assumed to be quasi-static, i.e., the CIR can be assumed constant for

the duration of a time slot. This is due to the fact that the coherence time of the channel (even for highway speeds of 60mph) is much larger than the slot duration of $577\mu\text{sec}$. This eliminates the need for channel tracking at the receiver. In addition, we assume that the fading process is independent between bursts. Furthermore, we assume two transmit antennas, an 8-PSK signal constellation with a symbol rate of 271 Ksymbols/sec, and the basic EDGE frame structure. Each burst consists of 26 training symbols used for channel impulse response estimation followed by 114 data symbols. Tail symbols are inserted to indicate the end of each burst and finally ramp down to guard against multipath effects. A linearized GMSK transmit pulse shape is assumed and its impulse response is truncated to ± 2 symbols on both sides of the main symbol. Ideal low-pass Nyquist filtering is assumed at the receiver. The average profile of the overall discrete-time impulse response for a Typical Urban channel at 3km/h (TU3) (including the linearized GMSK pulse shape) consists of 5 taps. However, the 5th tap has an average energy of -50 dB compared to the largest tap. Therefore, the effect of this tap is ignored in the simulations. Perfect channel estimation is assumed at the receiver unless otherwise stated.

Figures 4 - 6 show the effect of the FEP on the performance of a delay diversity system employing two transmit and one receive antennas. The FEP is designed to shorten the equivalent 5-tap channel to 2 taps followed by an 8-state full MLSE equalizer. Figure 4 depicts the Bit Error Rate (BER) versus the receiver SNR for different FEP lengths. It is clear from this figure that the 8-state DDFSE without FEP has very poor performance on the TU3 channel. This is expected since the DDFSE in this case is implemented using an 8-state MLSE equalizer (i.e. the decoder memory is 1) with 3 decision feedback taps to cancel the residual ISI. The three taps used for feedback have a significant energy content, therefore, channel shortening is necessary to reduce the effect of error propagation due to feedback. This is evident by the significant reduction in BER achieved using the FEP. Figure 4 also shows that the effect of increasing the FEP length on BER becomes more noticeable at high SNR levels (where the effects of channel dispersion dominate) and an error floor is observed when a short FEP is used. This figure clearly demonstrates the critical role played by the FEP where we see that using a 16-tap FEP with an 8-state MLSE equalizer improves the receiver performance over the 64-state DDFSE without FEP by $\approx 2-2.5$ dB while reducing equalizer complexity by a factor of 8.

Next, we investigate the effect of the FEP on the uncoded and coded Block Error Rate (BLER) performance. Figure 5 shows that the improvement in BER does not result in a corresponding improvement in BLER. The higher uncoded BLER when the FEP is used indicates that corrupted blocks have fewer erroneous bits per block. On the other hand, fewer corrupted blocks with a higher number of erroneous bits are obtained using 64-state DDFSE without FEP since bit errors propagate due to feedback. Therefore, it is conjectured that the BLER can be reduced (at the expenses of some

throughput loss) significantly by applying a powerful outer error correcting block code (such as a Reed–Solomon code). This conjecture is verified in Figure 6 which shows the achievable coded BLER with a rate- $\frac{1}{3}$ outer code used in the transmitter to enable the error correction of up to one third of the block bit errors. For the rest of this section, we will concentrate on the BER as the performance measure when comparing different system structures.

Figure 7 shows the effect of the delay parameter Δ on both SSNR and BER for a 2–transmit 1–receive delay diversity system with a 32–tap FEP at different receiver SNR levels. It can be seen that the FEP performance is insensitive to Δ when it is chosen to be close to $N_f/2$. Therefore, the FEP computational complexity can be reduced dramatically by avoiding the step of searching for the optimum delay.

Figures 8 and 9 show the effect of the FEP on the performance of the 8–state 8–PSK STTC with 2 transmit and 1 receive antennas. Figure 8 shows that the BER is unacceptable if both channels are shortened to 2 taps and an 8–state DDFSE is used due to the feedback error propagation effect of the DDFSE. On the other hand, if both channels are shortened to 1 tap, the BER improves since an 8–state full MLSE equalizer is used which does not suffer from error propagation. Even better performance is obtained if the first channel is shortened to 2 taps while the second channel is shortened to only 1 tap. However, Figure 8 clearly shows that, even with an optimized FEP, using an 8–state equalizer for the STTC results in an error floor and worse performance than the 64–state DDFSE without FEP. Hence, for the STTC case, we focus on the 64–state equalizer and try to further improve its performance by adding a FEP. Such a result is depicted in Figure 9 where it can also be seen that the effect of changing the FEP length is very small for $N_f \geq 8$. The performance of the 64–state DDFSE (where each channel is shortened to 3 taps) is superior to that of the 64–state full MLSE equalizer (where each channel is shortened to 2 taps) for moderate–to–high receiver SNR levels. This indicates that in this case, the loss in performance due to prefiltering is higher than the loss from feedback. Adding an 8–tap FEP to the 64–state DDFSE further improves its performance by ≈ 2.5 –3 dB.

Next, we investigate the performance with 2 receive antennas. The BER versus receiver SNR results for the STTC using 2 transmit and 2 receive antennas with 8–state and 64–state equalizers are shown in Figures 10 and 11, respectively. Figure 10 shows that the performance of variable–length shortening (i.e. different N_b for the 2 channels) with an 8–state full MLSE equalizer is better than the 2–transmit 2–receive 64–state DDFSE without FEP for $\text{SNR} < 20\text{dB}$ (the improvement is 3 dB at $\text{BER}=10^{-2}$). Moreover, its performance is better than the 2–transmit 1–receive 64–state DDFSE without prefilter for all SNRs of interest (with improvement ≈ 8 dB at $\text{BER}=10^{-2}$). However, at high SNR levels, the BER of the 8–state equalizer with FEP exhibits an error floor which can be eliminated using a 64–state equalizer, as shown in Figure 11. This figures also shows that using a FEP with

the 64-state equalizer improves the performance by over 5 dB at BER=10⁻² at the the expense of implementing two 8-tap FIR prefilters.

All the results presented thusfar assumed perfect channel knowledge at the receiver. We investigated the effect of channel estimation errors on performance by using length-26 perfect root-of-unity sequences (PRUS) [13] for training and a least squares channel estimation algorithm [14]. The results are given in Figure 12 which shows that performance loss due to channel estimation is less than 1.5 dB both with and without a FEP. Finally, we illustrate the numerical accuracy advantage of including the noise term \mathbf{R}_{nn} in the FEP design criterion (c.f. Equation (13)). Consider the following EDGE channel realization ³ $\mathbf{h} = [0.0007 \quad 0.3255 \quad 0.5441 \quad 0.3065]$ with $N_f = 8$, $N_b = 2$, and $\Delta = 4$. In Figure 13, we plot the *condition number* ⁴[11] of the matrix \mathbf{A} , as defined in (13), as a function of the SNR level. It can be seen from the figure that the highest value assumed by the condition number is 1033.5 at the highest SNR level under consideration of 30 dB. Without including the noise term \mathbf{R}_{nn} , as done in [9, 10], the condition number of \mathbf{A} is equal to 3.7051×10^{22} ! This results in significant numerical precision problems and unreliable results when computing the FEP using (14).

5 Conclusions

We presented FIR prefilter design algorithms for DDFSE equalization of space-time-coded signaling over multipath-fading channels and applied them to the EDGE transmission environment. For delay diversity transmission, a single 16-tap prefilter reduced the equalizer complexity from 64 states to 8 states while improving performance by 2-2.5 dB. For the 8-state 8-PSK STTC, a single 8-tap prefilter preceding the 64-state DDFSE equalizer improves performance by an additional 2.5-3 dB. Even more dramatic performance gains were achieved using 2 receive antennas and 2 prefilters.

Acknowledgement

We would like to thank Dr. A. F. Naguib of Morphics Technology and Dr. A.R. Calderbank of AT&T Shannon Laboratory for their help and support throughout the course of this work.

References

- [1] TIA 45.5 Subcommittee. The CDMA 2000 Candidate Submission. Draft, June 1998.

³We would like to thank Dr. C. Fragouli for generating this example.

⁴The condition number of a matrix is equal to the ratio of its largest to smallest eigenvalue. A smaller condition number results in better finite-precision numerical behavior when performing matrix operations like inversion, Cholesky factorization, etc.

- [2] Texas Instruments. Space-Time Block Coded Transmit Antenna Diversity for WCDMA. SMG2 document 581/98, submitted October 1998.
- [3] G.D. Forney Jr. Maximum-Likelihood Sequence Estimation of Digital Sequences in the Presence of Intersymbol Interference. *IEEE Transactions on Information Theory*, 18(3):363–378, May 1972.
- [4] A. Duel-Hallen and C. Heegard. Delayed Decision-Feedback Sequence Estimation. *IEEE Transactions on Communications*, pages 428–436, May 1989.
- [5] A. Naguib and N. Seshadri. MLSE and Equalization of Space-Time Coded Signals. In *VTC-Spring*, pages 1688–1693, May 2000.
- [6] V. Tarokh, N. Seshadri, and A.R. Calderbank. Space-Time Codes for High Data Rate Wireless Communications : Performance Criterion and Code Construction. *IEEE Transactions on Information Theory*, pages 744–765, March 1998.
- [7] V. Tarokh, A. Naguib, N. Seshadri, and A.R. Calderbank. Space-Time Codes for High Data Rate Wireless Communication : Performance Criteria in the Presence of Channel Estimation Errors, Mobility, and Multiple Paths. *IEEE Transactions on Communications*, pages 199–207, February 1999.
- [8] A. Naguib, V. Tarokh, N. Seshadri, and A.R. Calderbank. A Space-Time Coding Modem for High-Data-Rate Wireless Communications. *IEEE Journal on Selected Areas in Communications*, pages 1459–1477, October 1998.
- [9] P. Melsa, R. Younce, and C. Rohrs. Impulse Response Shortening for Discrete MultiTone Transceivers. *IEEE Transactions on Communications*, pages 1662–1672, December 1996.
- [10] C. Yin and G. Yue. Optimal Impulse Response Shortening for Discrete Multitone Transceivers. *Electronic Letters*, pages 35–36, January 1998.
- [11] G. Golub and C. Van Loan. *Matrix Computations*. The Johns Hopkins University Press, 1989. Second Edition.
- [12] T. Kailath and A.H. Sayed. Displacement Structure: Theory and Applications. *SIAM Review*, 37(3):297–386, September 1995.
- [13] G. Caire and U. Mitra. Training Sequence Design for Adaptive Equalization of Multi-User Systems. In *Asilomar*, pages 1479–1483, 1998.

- [14] S. Crozier, D. Falconer, and S. Mahmoud. Least Sum of Squared Errors (LSSE) Channel Estimation. *IEE Proc. - Part F*, pages 371–378, August 1991.

Delay (μsec)	0.0	0.2	0.5	1.6	2.3	5.0
Strength (dB)	-3.0	0.0	-2.0	-6.0	-8.0	-10.0

Table 1: EDGE TU Channel Model

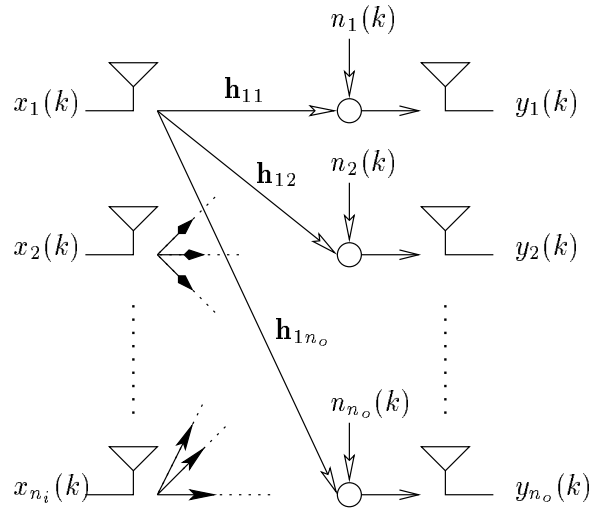


Figure 1: Block Diagram of the Multi-Input Multi-Output Channel Model

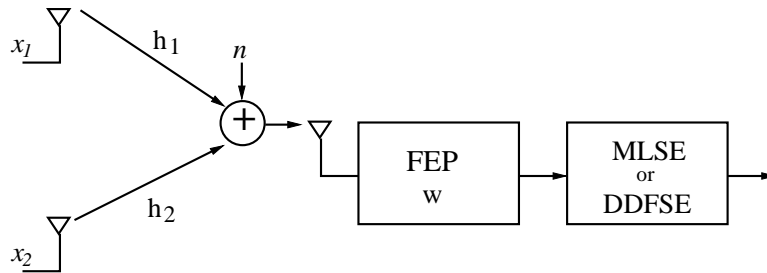


Figure 2: Receiver Structure for 2 Transmit and 1 Receive Antennas

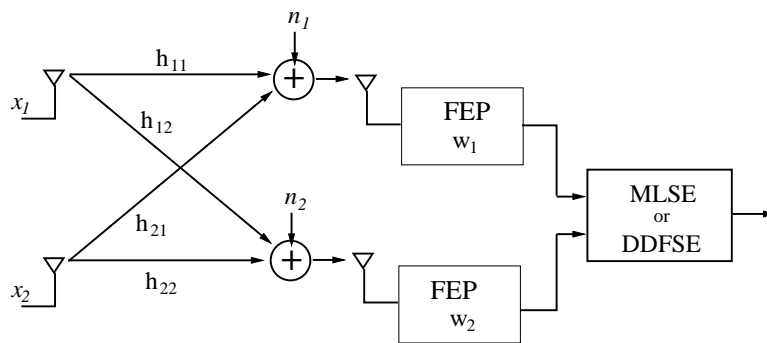


Figure 3: Receiver Structure for 2 Transmit and 2 Receive Antennas

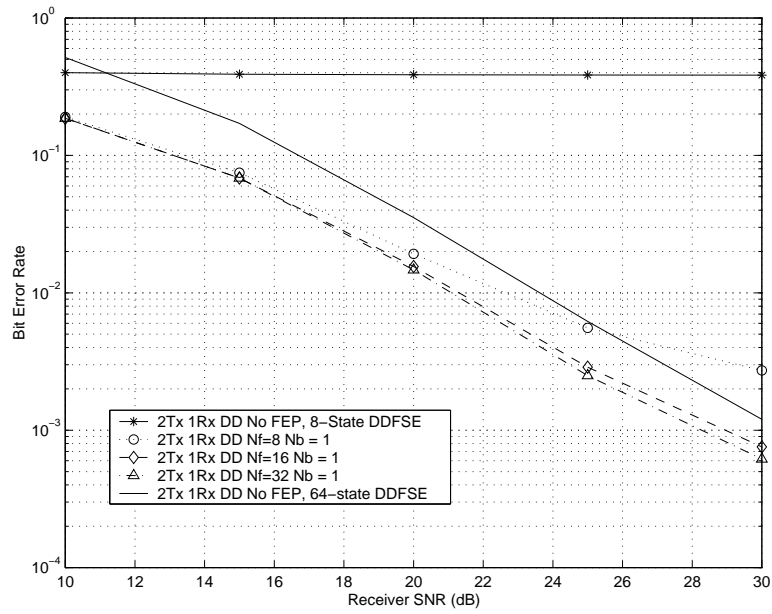


Figure 4: BER Performance of 2 Transmit 1 Receive Delay Diversity

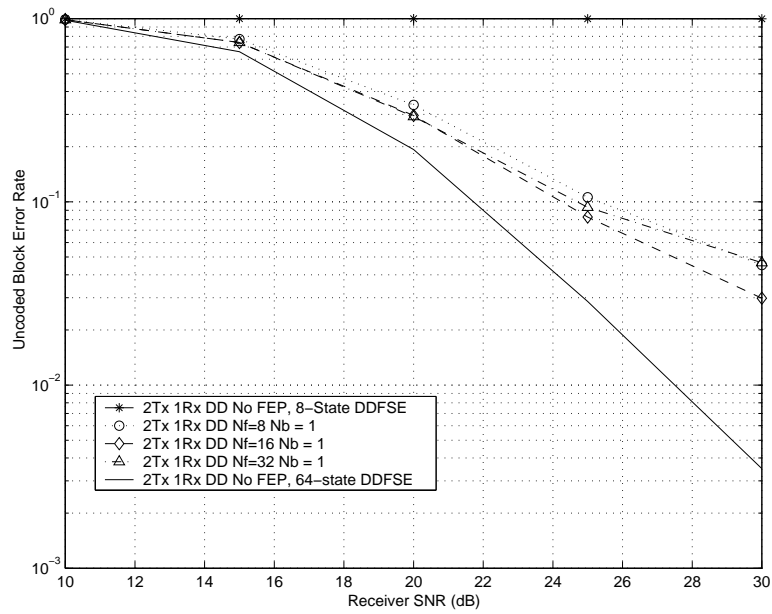


Figure 5: Uncoded BLER Performance of 2 Transmit 1 Receive Delay Diversity

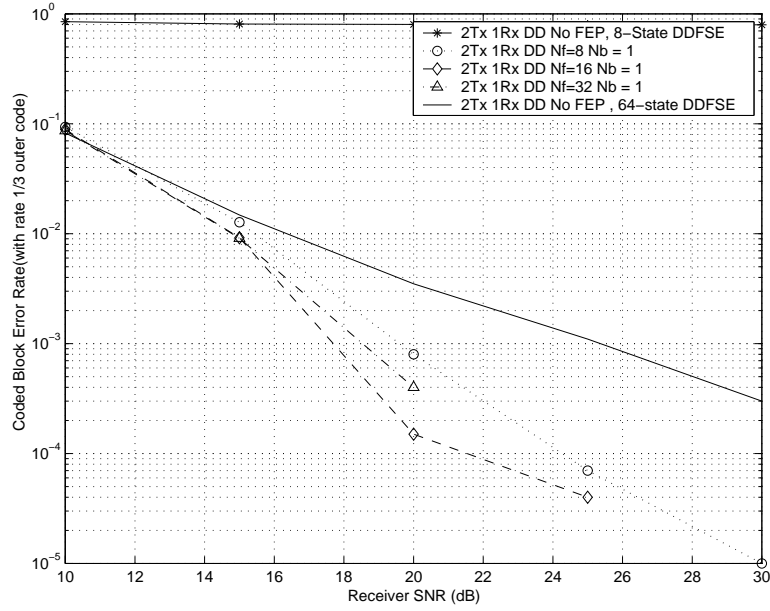


Figure 6: Coded BLER Performance of 2 Transmit 1 Receive Delay Diversity (with Rate= $\frac{1}{3}$ outer block code)

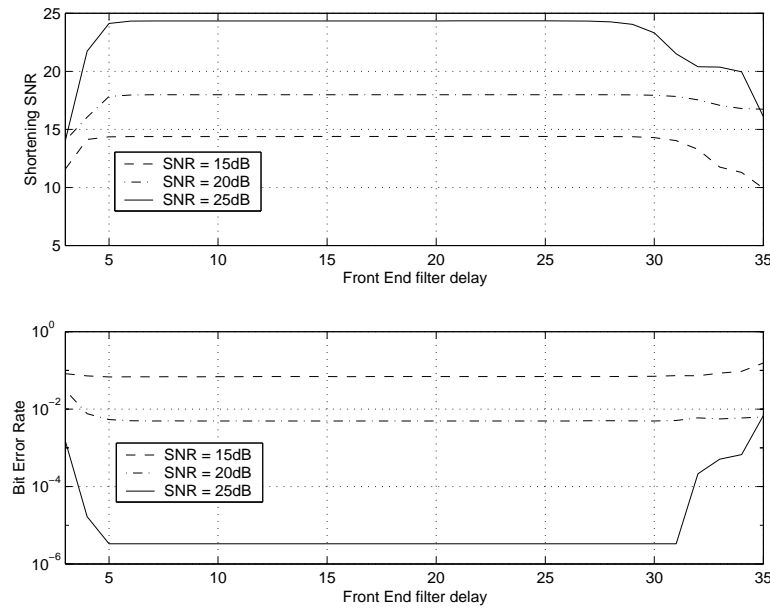


Figure 7: Effect of Delay Parameter on Shortening SNR and BER

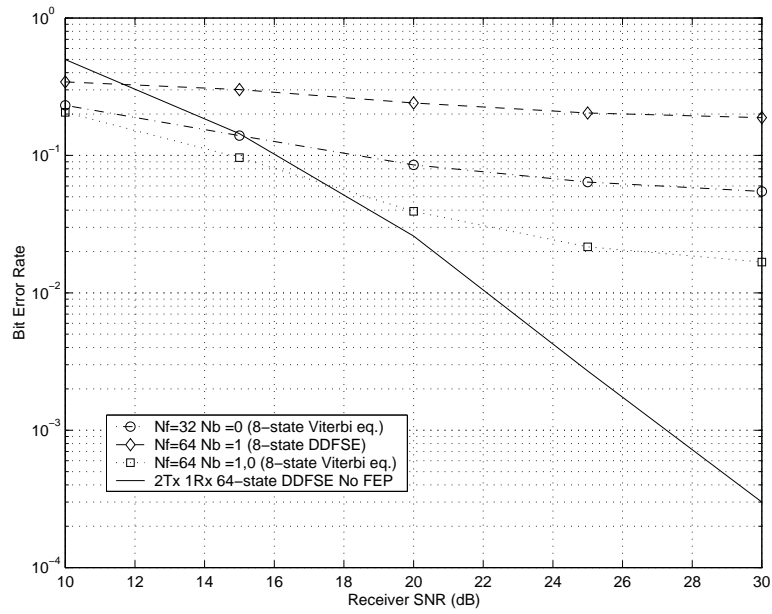


Figure 8: BER Performance of 2 Transmit 1 Receive STTC with 8-state Equalizer

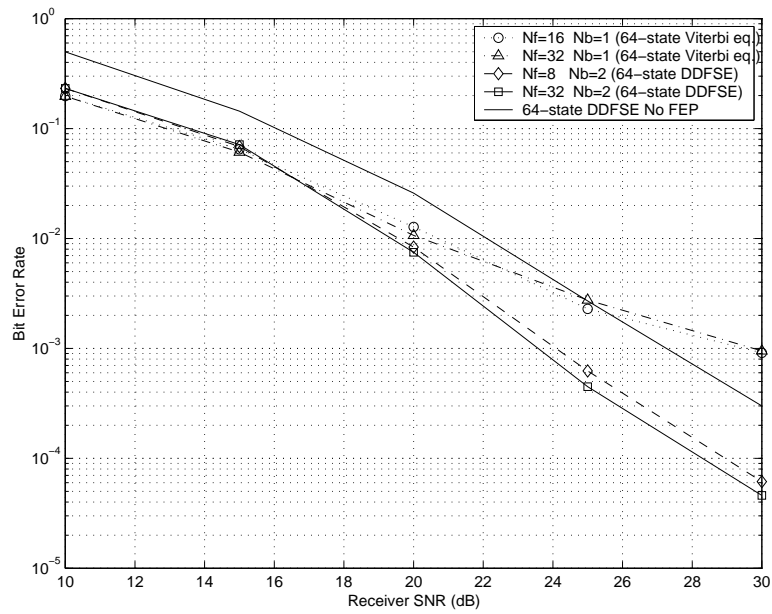


Figure 9: BER Performance of 2 Transmit 1 Receive STTC with 64-state Equalizer

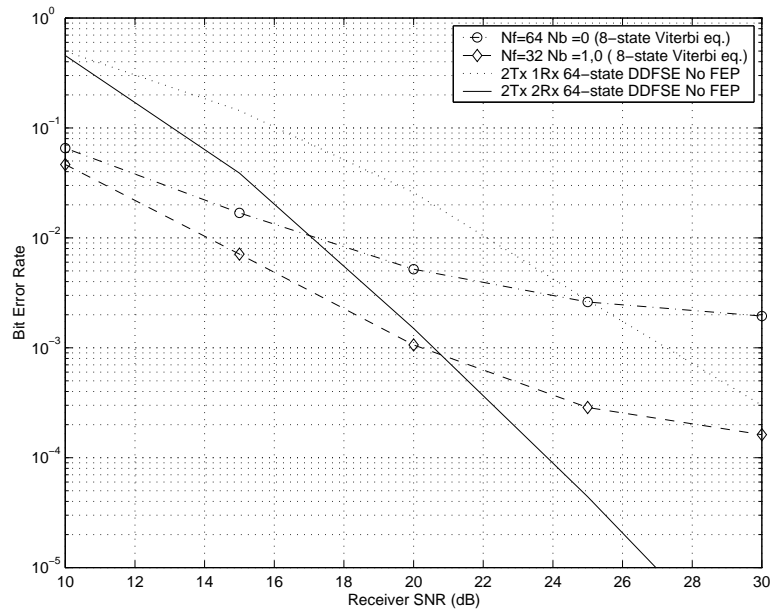


Figure 10: BER Performance of 2 Transmit 2 Receive STTC with 8-state Equalizer

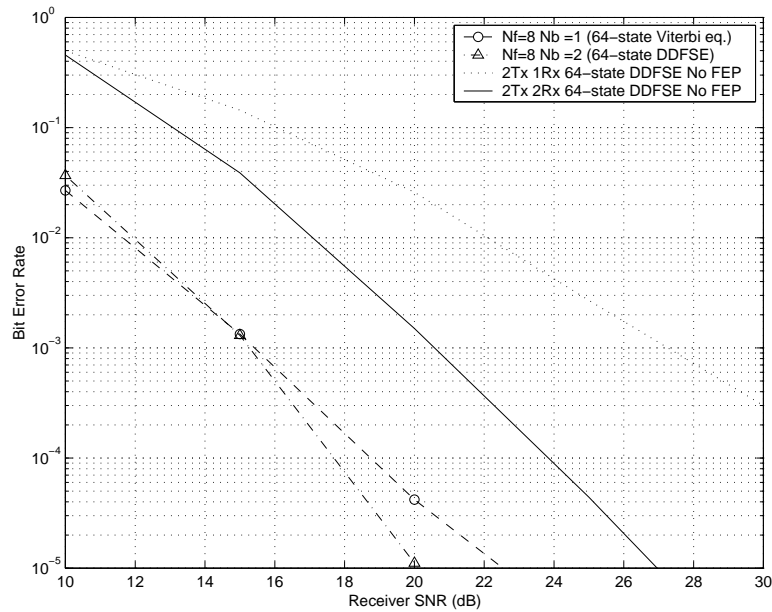


Figure 11: BER Performance of 2 Transmit 2 Receive STTC with 64-state Equalizer

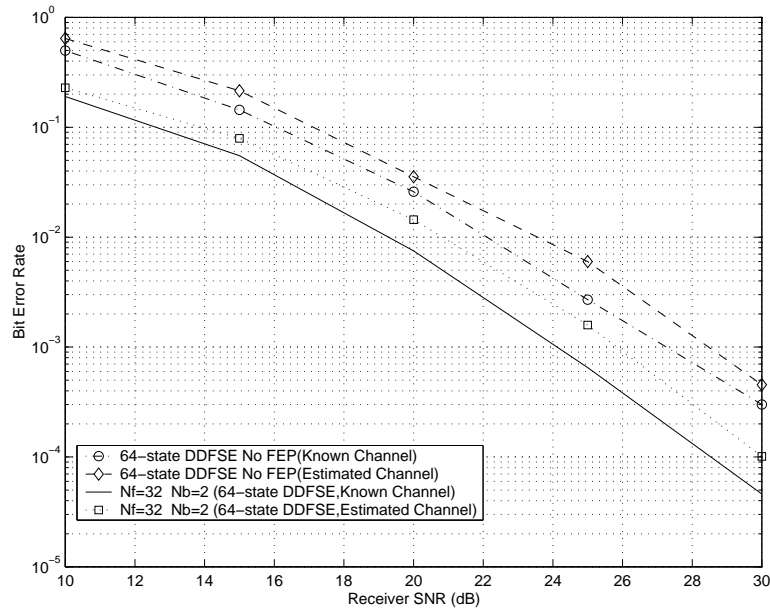


Figure 12: Effect of Channel Estimation Errors on Performance of 64-State DDFSE With and Without FEP for the 2 Transmit 1 Receive STTC Scenario

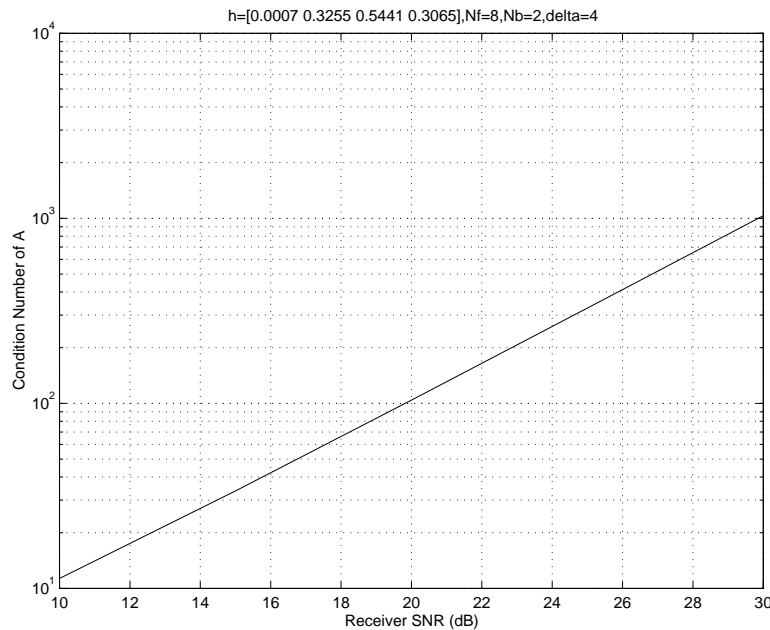


Figure 13: Condition Number of \mathbf{A} as defined in (13) as a Function of the SNR Level